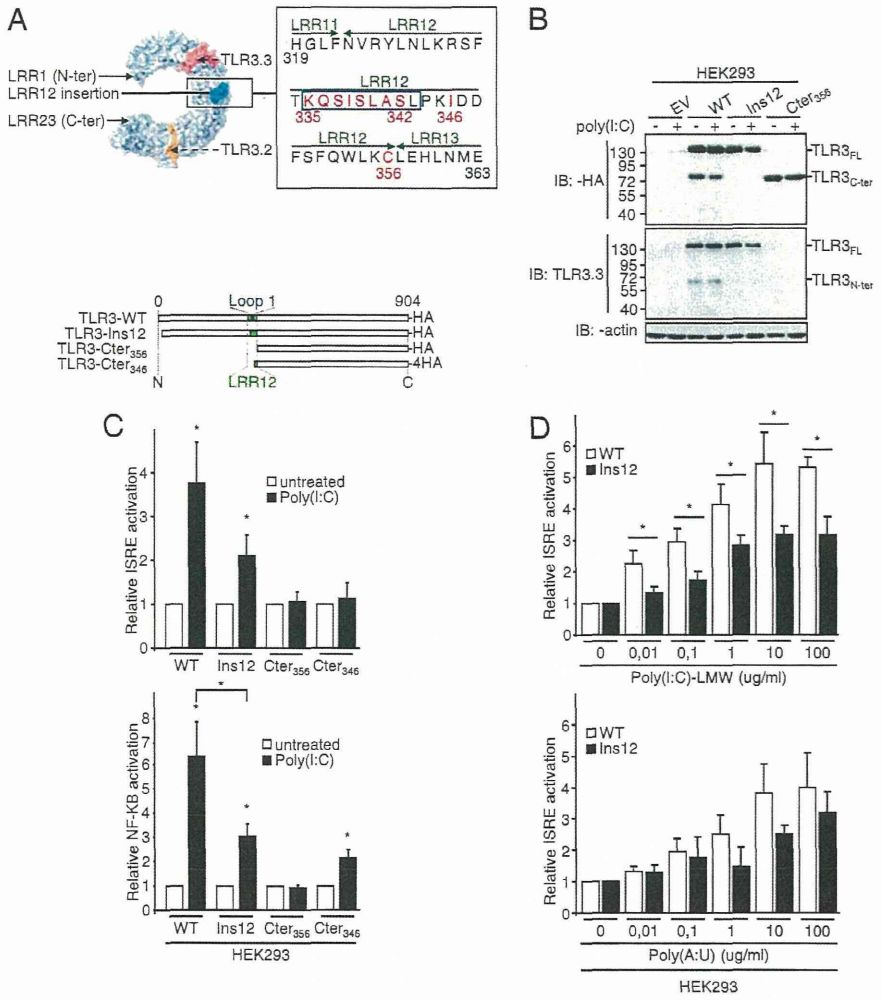

FIGURE 5. Noncleaved TLR3 can signal but the isolated C-terminal TLR3 fragment cannot. (**A**) *Upper panel*, Model of the putative location of the cleavage on LRR12 and TLR3 sequence with starting points of TLR3-$Cter_{356}$ and TLR3-$Cter_{346}$ mutants and deleted sequence (aa 335–342) of TLR3-Ins12 (in red). Blue framework: LRR12 loop1. *Lower panel*, Schematic representation of TLR3 mutants. (**B**) Immunoblot analysis of HEK293 cells transfected with empty vector (EV), TLR3-WT-HA (WT), TLR3-Ins12-HA (Ins12), or TLR3-$Cter_{356}$-HA ($Cter_{356}$) and then treated without (−) or with (+) Poly(I:C) (10 μg/ml) for 4 h. Lysates were analyzed with anti-HA, TLR3.3, and anti-actin Abs. Values represent molecular mass (kDa). (**C**) ISRE (*upper panel*) and NF-KB (*lower panel*) reporter assay in HEK293 cells transfected with TLR3-WT-HA, TLR3-Ins12-HA, TLR3-$Cter_{356}$-HA ($Cter_{356}$), or TLR3-$Cter_{346}$-HA ($Cter_{346}$), and then treated without (white) or with (black) Poly(I:C) (10 μg/ml) for 6 h. (**E**) ISRE reporter assay in HEK293 cells transfected with TLR3-WT-HA or TLR3-Ins12-HA and then treated with the indicated concentrations of Poly(I:C)-LMW or Poly(A:U) for 6 h. Data are representative (B) or the mean (C, D) of at least three independent experiments. Error bars (C, D) represent SEM. $*p < 0.05$, untreated versus Poly(I:C)-treated cells or response of TLR3-WT versus mutant TLR3.

but with significantly reduced efficiency for NF-κB compared with WT TLR3. In contrast, TLR3-$Cter_{356}$-HA was unable to activate either pathway, and TLR3-$Cter_{346}$-HA triggered a weak NF-κB response but no ISRE-dependent response. We next compared the levels of ISRE-dependent transcription in response to increasing concentrations of either LMW Poly(I:C) or Poly(A:U). The dose responses showed that HEK293 cells transfected with WT TLR3 were also significantly more sensitive to LMW Poly(I:C) but not to Poly(A:U) (Fig. 5D). Notably, both C-terminal fragments of the receptor were completely unresponsive to all doses of these two ligands (data not shown). Taken together, these results show that, in agreement with previous reports, uncleaved TLR3 can generate a response to dsRNA (30), whereas the isolated C-terminal fragment triggers only a weak signal (26).

The N- and C-terminal fragments of TLR3 remain associated after cleavage

Because cleaved TLR3 was able to signal in the total absence of $TLR3_{FL}$ (Fig. 4A, 4B, Supplemental Fig. 4A, 4B), whereas isolated $TLR3_{C\text{-}ter}$ was almost ineffective (Fig. 5C), we wondered whether the two fragments of TLR3 could remain associated after proteolytic cleavage. Therefore, we compared the profiles of TLR3 on Western blot performed with lysates prepared in nondenaturing (protein lysate neither reduced nor heated) versus denaturing conditions (Fig. 6A–D, Supplemental Fig. 4C). In nondenaturing conditions, we detected the 130 kDa band, whereas bands corresponding to the proteolytic fragments were barely detectable in epithelial NCI-H292 cells (Fig. 6A, Supplemental Fig. 4C), in mDCs (Fig. 6B), as well as in HEK293-TLR3-HA cells (Fig. 6C, 6D). We ensured that nondenaturing conditions did not prevent the migration of TLR3 fragments, because the constructs corresponding to the cleaved $TLR3_{C\text{-}ter}$ fragment ($Cter_{356}$ and $Cter_{346}$) migrated at expected molecular mass (~72 kDa; Fig. 6D). In contrast, when the same lysates were analyzed in denaturing conditions, $TLR3_{C\text{-}ter}$ and $TLR3_{N\text{-}ter}$ became clearly visible (Fig. 6A–D, Supplemental Fig. 4C), thereby revealing the presence of both uncleaved and cleaved/associated TLR3 in cells. Similarly, when nondenatured lysates were immunoblotted after running on a native gel, the same high molecular band was observed, with HEK293 cells expressing either WT or noncleavable TLR3 and with epithelial cells expressing endogenous TLR3 (Supplemental Fig. 4D). In contrast, the $TLR3_{C\text{-}ter}$ mutant migrated on the same gel at a much lower molecular mass. Moreover, nondenaturing conditions showed that Poly(I:C) treatment did not dissociate $TLR3_{C\text{-}ter}$ and $TLR3_{N\text{-}ter}$ (Fig. 6A–C, Supplemental Fig. 4C). To definitely confirm the association of the two cleaved fragments, we performed immunoprecipitation with C-terminal–specific TLR3.2 and N-terminal–specific TLR3.3 Abs and analyzed the precipitates by immunoblot with the two Abs. In all cases, $TLR3_{N\text{-}ter}$ and $TLR3_{C\text{-}ter}$ coimmunoprecipitated both in NCI-H292 cells (Fig. 6E) and HEK293-TLR3-HA cells (Fig. 6F). Lastly, reprecipitation after denaturation of the immunoprecipitates ob-

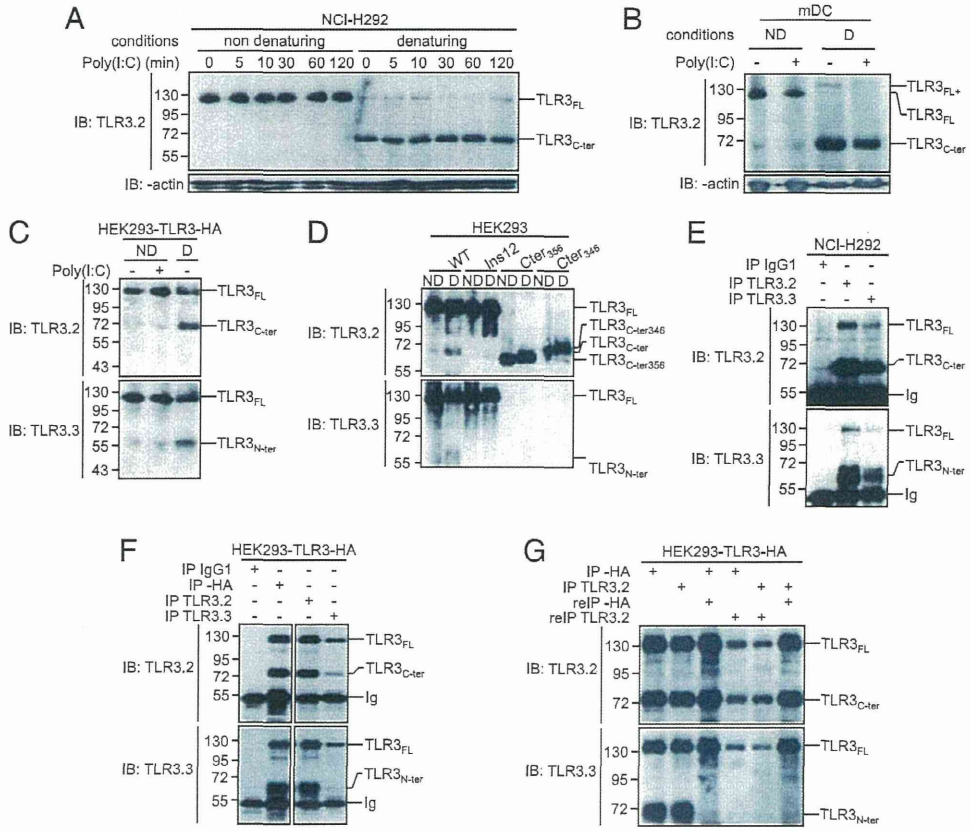

FIGURE 6. The N- and C-terminal fragments of endogenous TLR3 fragments remain associated after cleavage. (**A**) Immunoblot analysis of NCI-H292 cells treated with Poly(I:C) (10 μg/ml) for the indicated times. Lysates were denatured (D) or not (ND) and then analyzed with TLR3.2 and anti-actin Abs. (**B**) Immunoblot analysis of mDCs treated (+) or not (−) with Poly(I:C) (10 μg/ml) for the indicated times. Lysates were denatured (D) or not (ND) and then analyzed with TLR3.2 and anti-actin Abs. (**C**) Immunoblot analysis of HEK293-TLR3-HA cells treated (+) or not (−) with Poly(I:C) (10 μg/ml) for 2 h. Lysates were denatured (D) or not (ND) and then analyzed with TLR3.2 and TLR3.3 Abs. (**D**) Immunoblot analysis of HEK293 cells transfected with TLR3-WT-HA (WT), TLR3-Ins12-HA (Ins12), TLR3-Cter$_{356}$-HA (Cter$_{356}$), or TLR3-Cter$_{346}$-HA (Cter$_{346}$). Lysates were denatured (D) or not (ND) and then analyzed with TLR3.2 and TLR3.3 Abs. (**E**) Immunoblot analysis of NCI-H292 cells. Lysates were immunoprecipitated with IgG1, TLR3.2, or TLR3.3 Abs and analyzed with TLR3.2 and TLR3.3 Abs. (**F**) Immunoblot analysis of HEK293-TLR3-HA cells. Lysates were immunoprecipitated with IgG1, anti-HA, TLR3.2, or TLR3.3 Abs and analyzed with TLR3.2 and TLR3.3 Abs. (**G**) Immunoblot analysis of HEK293-TLR3-HA cells. Lysates were immunoprecipitated with anti-HA or TLR3.2 Abs and then precipitates were reimmunoprecipitated with anti-HA or TLR3.2 Abs and analyzed with TLR3.2 and TLR3.3 Abs. Values represent molecular mass (kDa). Data are representative of at least three independent experiments.

tained with a C-terminal–specific Ab (either TLR3.2 or anti-HA) led to the loss of the N-terminal fragment of TLR3, confirming that the association of the two fragments was through a noncovalent bond (Fig. 6G). Taken together, our data show that the two fragments of TLR3 remain associated after cleavage and that ligand binding does not disrupt this association (Fig. 7). Therefore, the cleaved/associated TLR3 represents the relevant endogenous TLR3 responsible for the majority of immunological functions.

Discussion

Remarkable progress has been made recently in our understanding of the biology of nucleic acid–sensing TLR3, TLR7, and TLR9. Notably, various data now suggest a model in which exogenous nucleotides can be recognized with high sensitivity, whereas self-nucleotide–induced signaling and autoimmunity are prevented (3). Discrimination between nonself- and self-nucleotides appears to be facilitated by several levels of regulation. Recently, cleavage of TLR9 in endolysosomes was shown to be required for generating the C-terminal fragment of the receptor that binds dsDNA with high affinity and signals. Published data indicated that this mechanism might also apply to TLR3 and TLR7 (9, 22). However, our data allow us to propose an alternative model for TLR3 biology (Fig. 7), which reconciles two requisites: the need to restrict dsRNA recognition in endolysosomes (and therefore to expose the receptor to a proteolytic environment) to prevent autoreactivity, as described for other endosomal TLRs, and the requirement of the two ligand binding sites present on the ECD of TLR3—the first near the N terminus and the second close to the transmembrane region—to recognize dsRNA with high avidity. Several aspects of the trafficking and processing of TLR3 diverge from what has been described for other lysosomal TLRs (8, 10).

Building on previous observations, and supported by data that were published after the submission of our manuscript (26), our results allow improvement of our model of TLR3 biology. In contrast to TLR9, which was reported to reside principally in the ER in resting cells (32) and to reach the acidic compartments after stimulation by double-stranded DNA (5–7, 33), TLR3 is continuously exported to the Golgi and accumulates in the endolysosomal compartments where it undergoes a single cleavage by cathepsins, most likely within the short (9 aa) LRR12 external loop; however, the exact cleavage site remains unknown. In contrast, asparagine endopeptidase first cleaves the long (30 aa) LRR14–15 flexible loop of TLR9 that is secondarily trimmed by cathepsins (8–10, 34, 35). Strong conservation of the LRR12 ex-

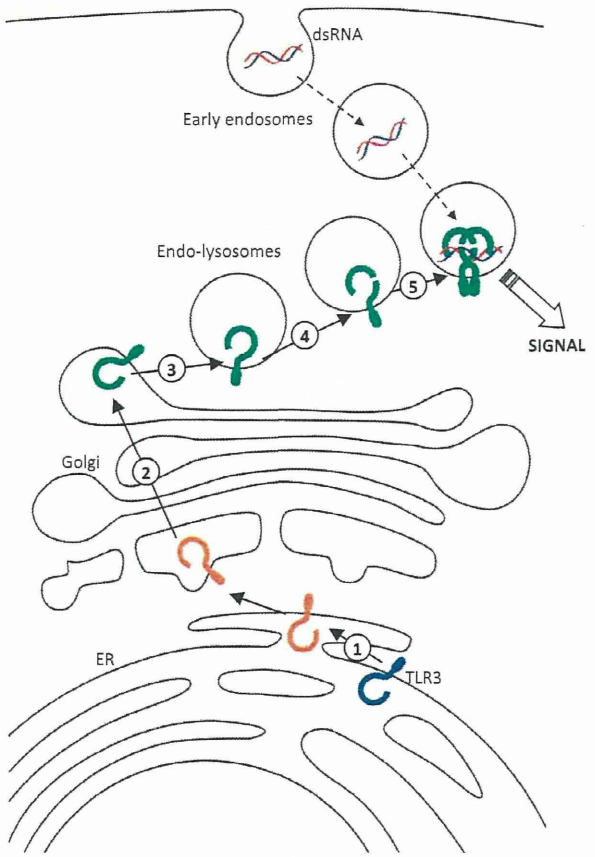

FIGURE 7. Proposed model of TLR3 processing. (**1**) TLR3 is neosynthesized and *N*-glycosylated in the ER. (**2**) Then, it crosses the Golgi apparatus where it is fully glycosylated to become EndoH resistant. TLR3 exits the Golgi to enter the endosome membrane (**3**) where it is cleaved by cathepsins (**4**). The two proteolytic fragments remain associated to fully signal (**5**).

ternal loop (residues 335–343) during mammals' evolution (30) suggests that cleavage is an important step in the biology of TLR3. Remarkably, our data confirm that the two proteolytic fragments of the ECD of TLR3 have prolonged half-lives (26) and demonstrate that they remain associated, suggesting that the noncovalent interactions between the adjacent LRRs known to stabilize the ECD of TLRs (36) have been preserved. Furthermore, the absence of detectable amounts of Golgi-modified $TLR3_{FL+}$ in resting immune and nonimmune cells (Figs. 1A, 1D–F, 3B, 3C) indicates that cleaved/associated TLR3 is the almost exclusive form of the receptor present in endolysosomes, where the encounter with exogenous dsRNA is known to occur (37). The lack of appropriate ligand prevented us from visualizing directly TLR3 bound to dsRNA. However, the physical association of TRIF with $TLR3_{C\text{-}ter}$, but not $TLR3_{FL}$, after activation with Poly(I:C) in NCI-H292 cells (38), combined with the absence of free $TLR3_{C\text{-}ter}$ in those cells, indicates that cleaved/associated TLR3 is the main form of the receptor recognizing Poly(I:C). The single cleavage, without further trimming, may explain why the two long-lived fragments of TLR3 remain associated to bind dsRNA. In contrast, although it was proposed that some TLR9 fragments could remain associated (8, 39), the C-terminal fragment of the receptor is viewed as the major form of the functional receptor, binding agonist CpG oligodesoxynucleotides with high affinity and being able to efficiently recruit the adaptor protein MyD88 (8, 10).

The streamlined transfer to endolysosomes, followed by rapid cleavage, explains why endogenous TLR3 fragments were abundant in resting cells of every type analyzed, whereas $TLR3_{FL}$ was difficult to detect. In contrast, comparable amounts of $TLR3_{FL}$ and TLR3 fragments were observed in HEK293 cells, suggesting an imbalance between the high expression of exogenous TLR3 and the availability of the chaperone protein Unc93b1 in those cells (26). Indeed, exogenous TLR3 was abundant in the ER, whereas endogenous TLR3 was found mostly in the endolysosomes. Moreover, the half-lives of the fragments from transfected TLR3 were shorter compared with endogenous TLR3 (compare Fig. 2B with Fig. 2A). These differences should be kept in mind when studying the biology of endosomal TLRs in HEK293 cells.

TLR3 cleavage could increase or decrease the sensitivity of the receptor and/or modify its specificity for different ligands. Our functional studies reveal that, in TLR3-transfected HEK293 cells, the cleavage increased the sensitivity to HMW and LMW Poly(I:C). The increased sensitivity of cleaved/associated TLR3 remains perplexing. Thus, cleavage could somehow increase the affinity of the ECD for its ligands or ease the conformational change that may occur in the presence of dsRNA (39) and that may facilitate the recruitment of TRIF. In agreement with Qi et al. (26), we observed that $TLR3_{C\text{-}ter}$ by itself was consistently unable to trigger a strong response to dsRNA. A difference in timing (6 versus 18 h) might explain, in part, the variance between those results and recently published data that showed an equal response to Poly(I:C) with either TLR3-WT or $TLR3_{C\text{-}ter}$ (22). Whatsoever the residual activity of $TLR3_{C\text{-}ter}$, its physiological importance is uncertain, because cleaved/associated TLR3 appears to be the predominant form of the endogenous receptor present in the endolysosomes where recognition of dsRNA takes place.

The central role of cleaved/associated TLR3 highlights the importance for dsRNA binding affinity and sensitive signaling of two distinct ligand-binding sites, each present on one proteolytic fragment. Moreover, the increased sensitivity to Poly(I:C) and the remarkable stability of this form of the receptor allows the reconciliation of some apparently discordant results from the literature. Indeed, one group reported the absence of inhibition of TNF production by RAW macrophages treated for 12 h with cathepsin inhibitors and then for 2 h with 100 μg/ml of Poly(I:C) (8), whereas another group showed a strong suppression of TNF production by the same cells in response to 1 μg/ml of Poly(I:C) (9). These different outcomes may be due to differences in the concentration of ligand used, with high concentrations of dsRNA being able to activate the less efficient $TLR3_{FL}$ in these cells. In addition, our data show that 12 h of Z-FA-fmk pretreatment is not sufficient to suppress the expression of TLR3 fragments in NSCLC cells, suggesting that the lack of inhibition by Z-FA-fmk of cells activated with moderate concentrations of Poly(I:C) could have resulted from the persistence of some cleaved/associated TLR3 at the time of stimulation.

In conclusion, TLR3 provides the first example, to our knowledge, of endosomal receptor maturation by cleavage followed by conversion into a functional cleaved/associated form of the protein. Considering that cleavage of WT-TLR3 is necessary for signaling, cleaved/associated TLR3 is the principal (and possibly exclusive) signaling receptor, and noncleavable TLR3 is able to signal, an intriguing conclusion of the present work is that the licensing consequence of TLR3 cleavage for signaling is not the separation of the two fragments. Further studies are required to fully evaluate the structural and functional consequences of TLR3 processing in vitro and in vivo, as well as to determine to what extent some aspects of TLR3 biology might apply to the other endolysosomal TLRs.

Acknowledgments

We thank Olivier Micheau (Bourgogne University, Dijon, France) for critical reading of the manuscript, Philippe Benaroch for reviewing the results and for the plasmid gift, and Sebastian Amigorena for discussions (both at Curie Institute, Paris, France).

Disclosures

The authors have no financial conflicts of interest.

References

1. Kawai, T., and S. Akira. 2011. Toll-like receptors and their crosstalk with other innate receptors in infection and immunity. *Immunity* 34: 637–650.
2. Gay, N. J., and M. Gangloff. 2007. Structure and function of Toll receptors and their ligands. *Annu. Rev. Biochem.* 76: 141–165.
3. Barton, G. M., and J. C. Kagan. 2009. A cell biological view of Toll-like receptor function: regulation through compartmentalization. *Nat. Rev. Immunol.* 9: 535–542.
4. Limmon, G. V., M. Arredouani, K. L. McCann, R. A. Corn Minor, L. Kobzik, and F. Imani. 2008. Scavenger receptor class-A is a novel cell surface receptor for double-stranded RNA. *FASEB J.* 22: 159–167.
5. Barton, G. M., J. C. Kagan, and R. Medzhitov. 2006. Intracellular localization of Toll-like receptor 9 prevents recognition of self DNA but facilitates access to viral DNA. *Nat. Immunol.* 7: 49–56.
6. Tabeta, K., K. Hoebe, E. M. Janssen, X. Du, P. Georgel, K. Crozat, S. Mudd, N. Mann, S. Sovath, J. Goode, et al. 2006. The Unc93b1 mutation 3d disrupts exogenous antigen presentation and signaling via Toll-like receptors 3, 7 and 9. *Nat. Immunol.* 7: 156–164.
7. Kim, Y.-M., M. M. Brinkmann, M.-E. Paquet, and H. L. Ploegh. 2008. UNC93B1 delivers nucleotide-sensing toll-like receptors to endolysosomes. *Nature* 452: 234–238.
8. Park, B., M. M. Brinkmann, E. Spooner, C. C. Lee, Y.-M. Kim, and H. L. Ploegh. 2008. Proteolytic cleavage in an endolysosomal compartment is required for activation of Toll-like receptor 9. *Nat. Immunol.* 9: 1407–1414.
9. Ewald, S. E., A. Engel, J. Lee, M. Wang, M. Bogyo, and G. M. Barton. 2011. Nucleic acid recognition by Toll-like receptors is coupled to stepwise processing by cathepsins and asparagine endopeptidase. *J. Exp. Med.* 208: 643–651.
10. Ewald, S. E., B. L. Lee, L. Lau, K. E. Wickliffe, G.-P. Shi, H. A. Chapman, and G. M. Barton. 2008. The ectodomain of Toll-like receptor 9 is cleaved to generate a functional receptor. *Nature* 456: 658–662.
11. Alexopoulou, L., A. C. Holt, R. Medzhitov, and R. A. Flavell. 2001. Recognition of double-stranded RNA and activation of NF-kappaB by Toll-like receptor 3. *Nature* 413: 732–738.
12. Casrouge, A., S.-Y. Zhang, C. Eidenschenk, E. Jouanguy, A. Puel, K. Yang, A. Alcais, C. Picard, N. Mahfoufi, N. Nicolas, et al. 2006. Herpes simplex virus encephalitis in human UNC-93B deficiency. *Science* 314: 308–312.
13. Zhang, S.-Y., E. Jouanguy, S. Ugolini, A. Smahi, G. Elain, P. Romero, D. Segal, V. Sancho-Shimizu, L. Lorenzo, A. Puel, et al. 2007. TLR3 deficiency in patients with herpes simplex encephalitis. *Science* 317: 1522–1527.
14. Guo, Y., M. Audry, M. Ciancanelli, L. Alsina, J. Azevedo, M. Herman, E. Anguiano, V. Sancho-Shimizu, L. Lorenzo, E. Pauwels, et al. 2011. Herpes simplex virus encephalitis in a patient with complete TLR3 deficiency: TLR3 is otherwise redundant in protective immunity. *J. Exp. Med.* 208: 2083–2098.
15. Matsumoto, M., H. Oshiumi, and T. Seya. 2011. Antiviral responses induced by the TLR3 pathway. *Rev. Med. Virol.* 21: 67–77.
16. Karikó, K., H. Ni, J. Capodici, M. Lamphier, and D. Weissman. 2004. mRNA is an endogenous ligand for Toll-like receptor 3. *J. Biol. Chem.* 279: 12542–12550.
17. Wang, Y., L. Liu, D. R. Davies, and D. M. Segal. 2010. Dimerization of Toll-like receptor 3 (TLR3) is required for ligand binding. *J. Biol. Chem.* 285: 36836–36841.
18. Bell, J. K., J. Askins, P. R. Hall, D. R. Davies, and D. M. Segal. 2006. The dsRNA binding site of human Toll-like receptor 3. *Proc. Natl. Acad. Sci. USA* 103: 8792–8797.
19. Liu, L., I. Botos, Y. Wang, J. N. Leonard, J. Shiloach, D. M. Segal, and D. R. Davies. 2008. Structural basis of toll-like receptor 3 signaling with double-stranded RNA. *Science* 320: 379–381.
20. Fukuda, K., T. Tsujita, M. Matsumoto, T. Seya, H. Sakiyama, F. Nishikawa, S. Nishikawa, and T. Hasegawa. 2006. Analysis of the interaction between human TLR3 ectodomain and nucleic acids. *Nucleic Acids Symp. Ser. (Oxf)* 50: 249–250.
21. Watanabe, T., T. Tokisue, T. Tsujita, M. Matsumoto, T. Seya, S. Nishikawa, T. Hasegawa, and K. Fukuda. 2007. N-terminal binding site in the human toll-like receptor 3 ectodomain. *Nucleic Acids Symp. Ser. (Oxf)* 51: 405–406.
22. Garcia-Cattanco, A., F. X. Gobert, M. Müller, F. Toscano, M. Flores, A. Lescure, E. Del Nery, and P. Benaroch. 2012. Cleavage of Toll-like receptor 3 by cathepsins B and H is essential for signaling. *Proc. Natl. Acad. Sci. USA* 109: 9053–9058.
23. Takada, E., S. Okahira, M. Sasai, K. Funami, T. Seya, and M. Matsumoto. 2007. C-terminal LRRs of human Toll-like receptor 3 control receptor dimerization and signal transmission. *Mol. Immunol.* 44: 3633–3640.
24. Sun, J., K. E. Duffy, C. T. Ranjith-Kumar, J. Xiong, R. J. Lamb, J. Santos, H. Masarapu, M. Cunningham, A. Holzenburg, R. T. Sarisky, et al. 2006. Structural and functional analyses of the human Toll-like receptor 3. Role of glycosylation. *J. Biol. Chem.* 281: 11144–11151.
25. Kaiser, W. J., J. L. Kaufman, and M. K. Offermann. 2004. IFN-α sensitizes human umbilical vein endothelial cells to apoptosis induced by double-stranded RNA. *J. Immunol.* 172: 1699–1710.
26. Qi, R., D. Singh, and C. C. Kao. 2012. Proteolytic processing regulates Toll-like receptor 3 stability and endosomal localization. *J. Biol. Chem.* 287: 32617–32629.
27. Chockalingam, A., J. C. Brooks, J. L. Cameron, L. K. Blum, and C. A. Leifer. 2009. TLR9 traffics through the Golgi complex to localize to endolysosomes and respond to CpG DNA. *Immunol. Cell Biol.* 87: 209–217.
28. Bell, J. K., I. Botos, P. R. Hall, J. Askins, J. Shiloach, D. M. Segal, and D. R. Davies. 2005. The molecular structure of the Toll-like receptor 3 ligand-binding domain. *Proc. Natl. Acad. Sci. USA* 102: 10976–10980.
29. Choe, J., M. S. Kelker, and I. A. Wilson. 2005. Crystal structure of human toll-like receptor 3 (TLR3) ectodomain. *Science* 309: 581–585.
30. Ranjith-Kumar, C. T., W. Miller, J. Xiong, W. K. Russell, R. Lamb, J. Santos, K. E. Duffy, L. Cleveland, M. Park, K. Bhardwaj, et al. 2007. Biochemical and functional analyses of the human Toll-like receptor 3 ectodomain. *J. Biol. Chem.* 282: 7668–7678.
31. Botos, I., L. Liu, Y. Wang, D. M. Segal, and D. R. Davies. 2009. The toll-like receptor 3:dsRNA signaling complex. *Biochim. Biophys. Acta* 1789: 667–674.
32. Leifer, C. A., M. N. Kennedy, A. Mazzoni, C. Lee, M. J. Kruhlak, and D. M. Segal. 2004. TLR9 is localized in the endoplasmic reticulum prior to stimulation. *J. Immunol.* 173: 1179–1183.
33. Latz, E., A. Schoenemeyer, A. Visintin, K. A. Fitzgerald, B. G. Monks, C. F. Knetter, E. Lien, N. J. Nilsen, T. Espevik, and D. T. Golenbock. 2004. TLR9 signals after translocating from the ER to CpG DNA in the lysosome. *Nat. Immunol.* 5: 190–198.
34. Kasperkovitz, P. V., M. L. Cardenas, and J. M. Vyas. 2010. TLR9 is actively recruited to *Aspergillus fumigatus* phagosomes and requires the N-terminal proteolytic cleavage domain for proper intracellular trafficking. *J. Immunol.* 185: 7614–7622.
35. Sepulveda, F. E., S. Maschalidi, R. Colisson, L. Heslop, C. Ghirelli, E. Sakka, A.-M. Lennon-Duménil, S. Amigorena, L. Cabanie, and B. Manoury. 2009. Critical role for asparagine endopeptidase in endocytic Toll-like receptor signaling in dendritic cells. *Immunity* 31: 737–748.
36. Manavalan, B., S. Basith, and S. Choi. 2011. Similar structures but different roles – an updated perspective on TLR structures. *Front. Physiol.* 2: 41.
37. de Bouteiller, O., E. Merck, U. A. Hasan, S. Hubac, B. Benguigui, G. Trinchieri, E. E. Bates, and C. Caux. 2005. Recognition of double-stranded RNA by human toll-like receptor 3 and downstream receptor signaling requires multimerization and an acidic pH. *J. Biol. Chem.* 280: 38133–38145.
38. Estornes, Y., F. Toscano, F. Virard, G. Jacquemin, A. Pierrot, B. Vanbervliet, M. Bonnin, N. Lalaoui, P. Mercier-Gouy, Y. Pachéco, et al. 2012. dsRNA induces apoptosis through an atypical death complex associating TLR3 to caspase-8. *Cell Death Differ.* 19: 1482–1494.
39. Li, Y., I. C. Berke, and Y. Modis. 2012. DNA binding to proteolytically activated TLR9 is sequence-independent and enhanced by DNA curvature. *EMBO J.* 31: 919–931.

Supplemental material

SUPPLEMENTAL FIGURE 1. (**A**) Fluorescence intensity profiles of HEK293-TLR3-HA cells stained with anti-HA and TLR3.1 antibodies. (**B**) Immunoblot analysis of THP1 and U937 cells; lysates were analyzed with TLR3.2 and anti-actin antibodies. Immunoblot analysis of U937 cells treated or not for 24 h with IFN (1000 IU/ml); lysates were analyzed with TLR3.2 and anti-actin antibodies. (**C**) Immunoblot analysis of U937 cells treated (+) or not (-) for 24 h with IFN (1000 IU/ml); lysates were analyzed with TLR3.2 and anti-actin antibodies, as indicated. (**D**) Immunoblot analysis of BEAS-2B cells treated (+) or not (-) for 24 h with IFN (1000 IU/ml); lysates were analyzed with TLR3.2, TLR3.3 and anti-actin antibodies. (**E**) Measurement of NF-KB and ISRE activation with luciferase-based reporter assays in THP1 cells treated or not (-) for 4 h with Poly(I:C) at indicated concentrations (left panel), with TNF-α (50 ng/ml) and with IFN-α (1000 IU/ml). Values represent molecular mass (kDa) (**B-D**). Data are representative (**A-D**) or mean (**E**) of three independent experiments. Error bars represent SEM.

SUPPLEMENTAL FIGURE 2. (**A**) Cytokine production in NCI-H1703 and NCI-H292 cells treated or not with Poly(I:C) (100 ug/ml) for 24 h. (**B**) ISRE reporter assay and immunoblot analysis in NCI-H292 and NCI-H1703 cells after non silencing (-) or TRIF (+) siRNAs transfections (20 uM) and treatment without (white) or with (black) Poly(I:C) (10 ug/ml) for 4 h. For immunoblot, lysates were analyzed with anti-TRIF

and anti-actin antibodies. *: $p < 0.05$ comparing untreated with Poly(I:C)-treated conditions. (**C**) Immunoblot analysis of NCI-H1703 cells treated during indicated times with Z-FA-fmk (20 uM) renewed every 24h. Lysates were analyzed with TLR3.2, TLR3.3 and anti-actin antibodies. (**D**) NF-KB (left panel) and ISRE (right panel) reporter assay in NCI-H292 cells pretreated during indicated times with Z-FA-fmk (20 uM) renewed every 24h, and then treated with Poly(I:C) (10 ug/ml) for 4 h. (**E**) NF-KB (left panel) and ISRE (right panel) reporter assay in NCI-H1703 cells pretreated during indicated times with Z-FA-fmk (20 uM) renewed every 24h, and then treated with Poly(I:C) (10 ug/ml) for 4 h. (**F**) Immunoblot analysis of U937 and NCI-H292 cells treated during indicated times with Z-FA-fmk (20 uM). Lysates were analyzed with TLR3.2 and anti-actin antibodies. (**G**) Immunoblot analysis of NCI-H1703 cells treated during indicated times with chloroquine (1 ug/ml). Lysates were analyzed with TLR3.2, TLR3.3 and anti-actin antibodies. Values represent molecular mass (kDa) (**B**, **C, F** and **G**). Data are representative (**C, F** and **G**) or mean (**A**, **B**, **D** and **E**) of three independent experiments. Error bars represent SEM.

SUPPLEMENTAL FIGURE 3. Fluorescence intensity profiles of NCI-H292 cells treated during indicated times with Poly(I:C) (10 ug/ml) and then stained with Lamp1, EEA1 and/or TLR3.1 antibodies. Data are representative of three independent experiments.

SUPPLEMENTAL FIGURE 4. (**A**) Immunoblot analysis of NCI-H292 cells at indicated times after non-silencing (-) or TLR3 (+) siRNAs transfections (20 uM).

Lysates were analyzed with TLR3.3 and anti-actin antibodies. (**B**) NF-KB reporter assay in NCI-H292 cells at indicated times after non-silencing (-) or TLR3 (+) siRNAs transfections (20 uM) and treatment without or with Poly(I:C) (10 ug/ml) for 4 h. (**C**) Immunoblot analysis of NCI-H292 cells treated (+) or not (-) with Poly(I:C) (10 ug/ml) for 2 h. Lysates were denatured (D) or not (ND) and then analyzed with TLR3.2, TLR3.3 and anti-actin antibodies. (**D**) Immunoblot analysis on native gel of NCI-H292, NCI-H1703 and HEK293 cells transfected with empty vector (EV), TLR3WT-HA (WT), TLR3Ins12-HA (Ins12) or TLR3Cter356-HA (Cter356). Lysates were not denaturated and then analyzed with TLR3.2 and anti-HA antibodies. Values represent molecular mass (kDa). Data are representative (**A, C** and **D**) or mean (**B**) of three independent experiments. Error bars represent SEM.

3

Supplemental material

Toscano et al.

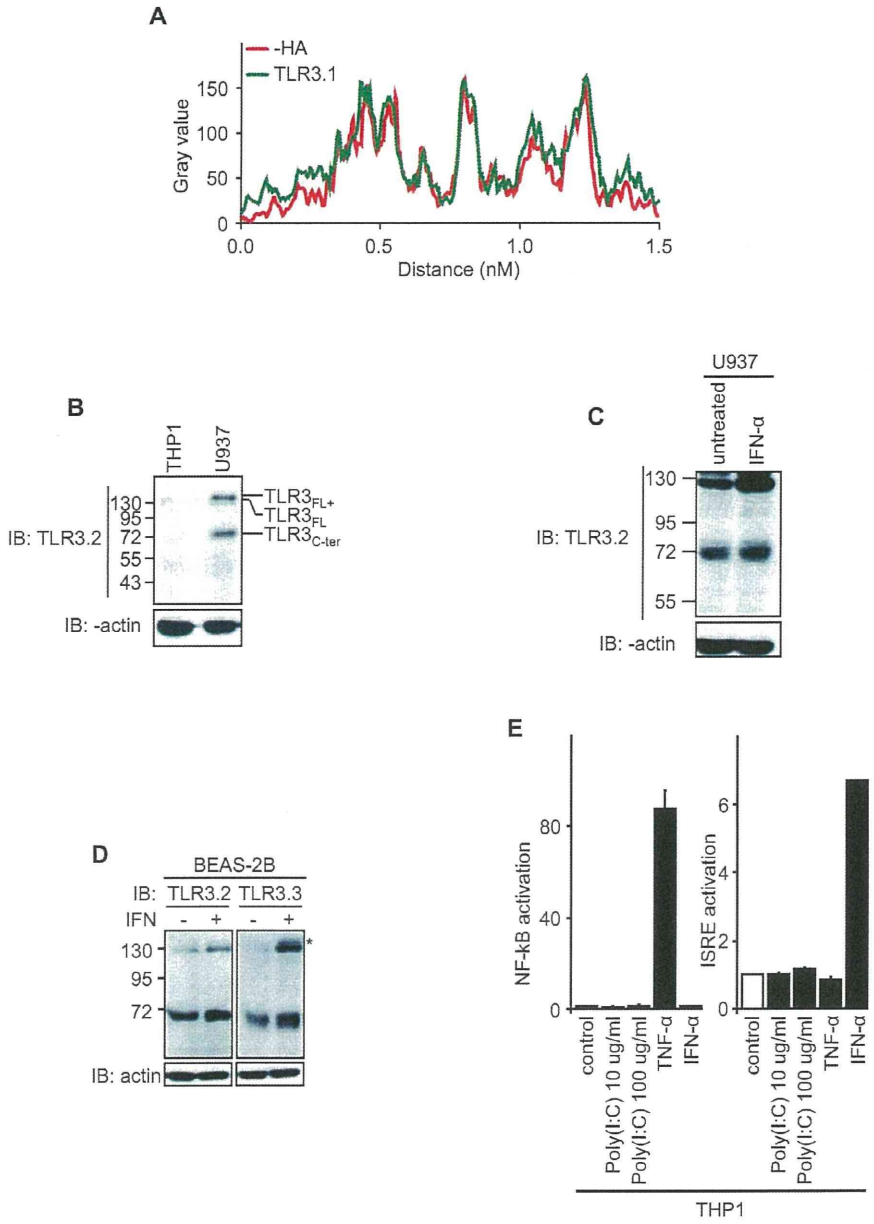

Figure 1

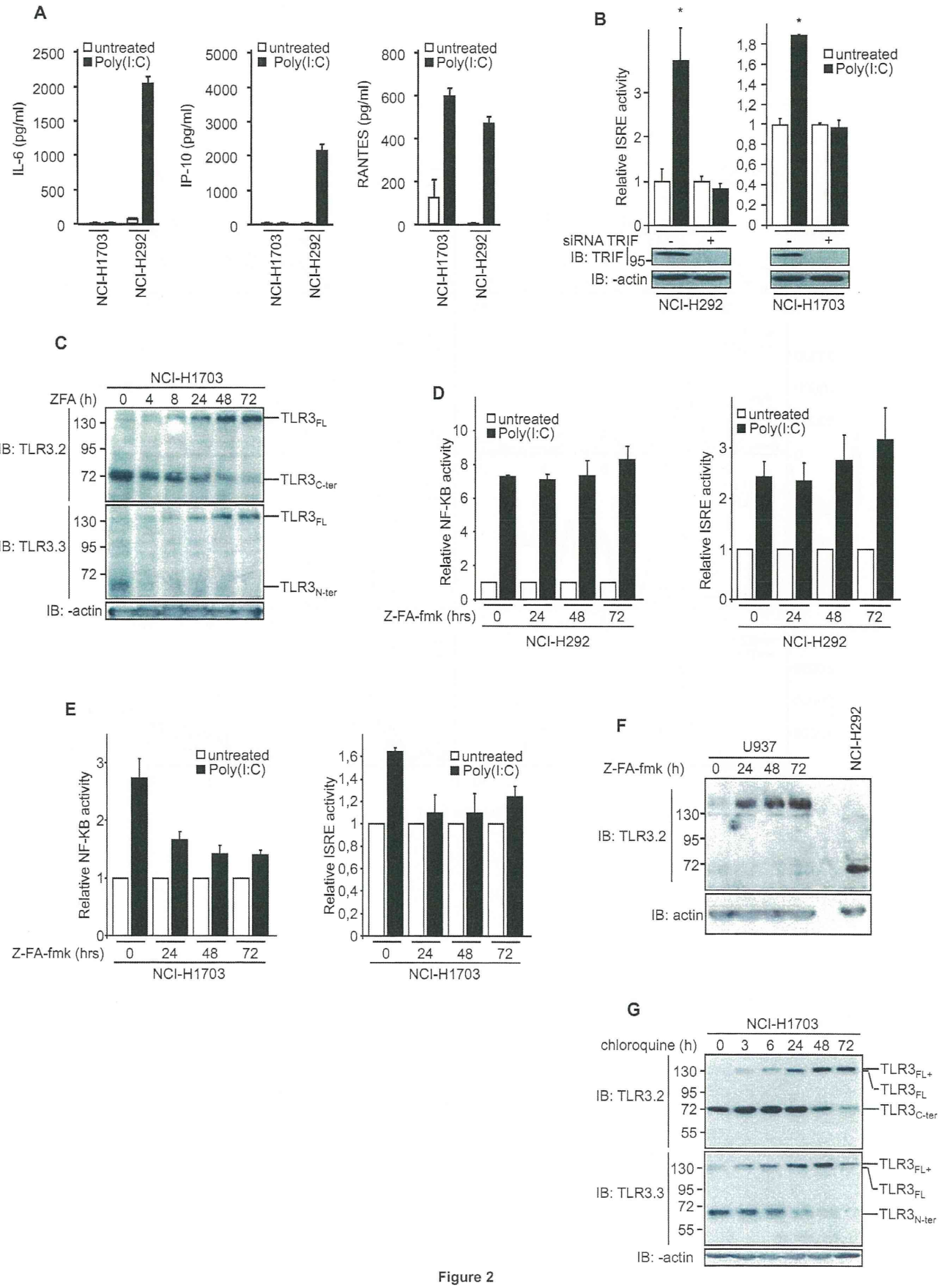
A
IL-6 (pg/ml)
IP-10 (pg/ml)
RANTES (pg/ml)
untreated
Poly(I:C)
NCI-H1703
NCI-H292
B
Relative ISRE activity
siRNA TRIF
IB: TRIF
IB: -actin
C
NCI-H1703
ZFA (h)
IB: TLR3.2
IB: TLR3.3
TLR3FL
TLR3C-ter
TLR3N-ter
D
Relative NF-KB activity
Relative ISRE activity
Z-FA-fmk (hrs)
E
F
U937
Z-FA-fmk (h)
IB: actin
G
chloroquine (h)
TLR3FL+

Figure 2

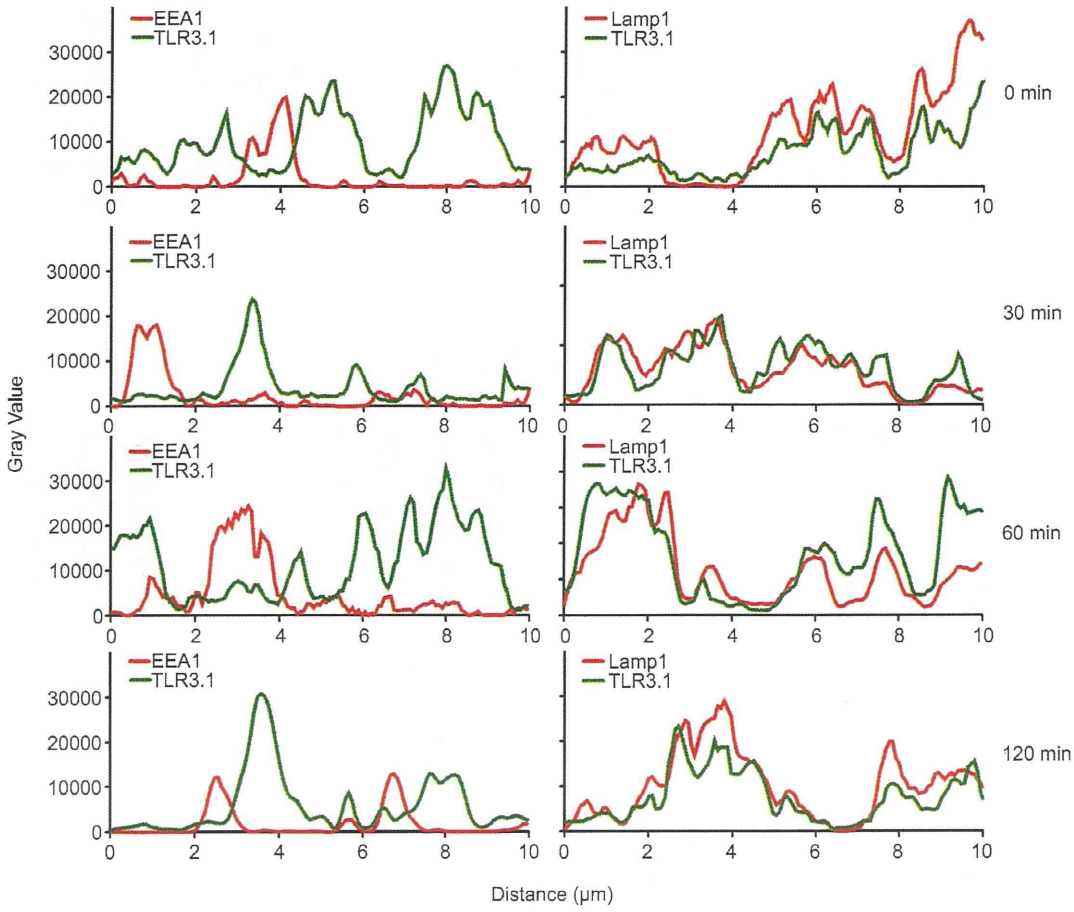
EEA1
TLR3.1
Lamp1
TLR3.1
0 min
30 min
60 min
120 min
Gray Value
Distance (μm)
0
10000
20000
30000
0
2
4
6
8
10

Figure 3